

# Vibrational Spectroscopic and Density Functional Studies on Ion Solvation and Association of Lithium Tetrafluoroborate in Acetonitrile

Xiaopeng Xuan,<sup>†,‡</sup> Hucheng Zhang,<sup>†,‡</sup> Jianji Wang,<sup>\*,†</sup> and Hanqing Wang<sup>‡</sup>

Department of Chemistry, Henan Normal University, Xinxiang, Henan 453002, P. R. China, and Lanzhou Institute of Chemical Physics, Chinese Academy of Sciences, Lanzhou, Gansu 73000, P. R. China

Received: June 21, 2004

Vibrational spectroscopic studies have been carried out on solutions of LiBF<sub>4</sub> in acetonitrile as a function of concentrations of lithium salt. Great changes in the vibrational characteristics of C≡N and C–C stretches were observed as a result of solvation. The solvation numbers of Li<sup>+</sup> determined from spectroscopic data are found to decrease from 3.2 to 1.4 with increasing concentration of the lithium salt. It is expected that the solvation number is 4 in the infinite diluted solution. Solvation structures of the lithium ion were suggested by density functional theory and the results were compared with the spectroscopic data. Changes of the  $\nu_1$  mode of BF<sub>4</sub><sup>−</sup> with concentration of the salt were also analyzed, and the bands at 763, 771, and 780 cm<sup>−1</sup> indicate the coexisting of free ion, contact ion pairs, and dimers. The structures of ion pairs in gas phase and in acetonitrile solutions were suggested on the basis of DFT calculations.

## Introduction

Lithium ion batteries have been widely applied to portable electronic devices in the recent decades due to their high density and low environmental impact. A typical lithium ion battery system is composed of a graphite anode, a transition metal oxide (such as LiMn<sub>2</sub>O<sub>4</sub>, LiNiO<sub>2</sub>) cathode, and a nonaqueous organic electrolyte. The most popular electrolytes in practice are mixtures of alkyl carbonates, for example, ethylene carbonate and propylene carbonate, and a lithium salt such as LiPF<sub>6</sub>. Unfortunately, the thermal instability and moisture sensitivity of LiPF<sub>6</sub> prevent its further applications.<sup>1</sup> It is, therefore, necessary to find a more stable lithium salt as an alternative of LiPF<sub>6</sub>. Among the commercially available lithium salts, LiBF<sub>4</sub> is known as a qualified salt, which can provide a proper and comparable electrolyte solution in terms of its chemical and thermal stabilities and electrochemical property.<sup>2</sup> However, LiBF<sub>4</sub> has not been used practically in lithium ion batteries because its electrolyte solution has a low ionic conductivity.<sup>2</sup> Therefore, it is very important to study the ion association and ion solvation in organic solutions, which have strongly negative effects on the improvement of conductivity by increasing the viscosity of solutions and decreasing the number of charge carriers.

Theoretical and experimental investigations of organic electrolyte solutions have been reported for improving the conductivity.<sup>3–11</sup> Among these investigations, conductance measurements of LiBF<sub>4</sub> in high dielectric constant solvents, such as propylene carbonate (PC)<sup>3,4</sup> and  $\gamma$ -butyrolactone (BL),<sup>5</sup> and in low dielectric constant solvents, including 2-methoxyethanol,<sup>6</sup> 2-methyltetrahydrofuran (2-MTHF),<sup>7</sup> 1,2-dimethoxyethane (DME),<sup>8,9</sup> and 1,2-dimethoxymethane (DMM),<sup>10</sup> have been reported. The medium to high level of ion pairs has been confirmed, even in high dielectric constant solvents. For

example, the dissociation degree of LiBF<sub>4</sub> in BL, with a salt concentration over 1.0 mol L<sup>−1</sup>, is only 34%.<sup>5</sup> The conductivity of LiBF<sub>4</sub> in DME<sup>7</sup> at 298.15 K shows that the Li<sup>+</sup> and BF<sub>4</sub><sup>−</sup> is strongly associated into contact ion pairs and triple ion pairs, even to dimers of the contact ion pair.

Despite the extensive attention devoted to the probe of ion–molecule and ion–ion interactions in solutions using vibrational spectroscopy, only very limited spectroscopic studies<sup>11–14</sup> were performed on the association of LiBF<sub>4</sub>. Alía and Edwards<sup>11</sup> studied the Raman spectra of LiBF<sub>4</sub> in acrylonitrile and found the presence of contact ion pairs and their dimers. Higher aggregation was also detected by infrared spectroscopy<sup>12,13</sup> in low dielectric constant solvents. No other details on structures of ion pairs such as Li<sup>+</sup>BF<sub>4</sub><sup>−</sup> were found in the literature.

The present work reports the vibrational spectroscopic and quantum chemistry studies on the ion solvation and ion association of LiBF<sub>4</sub> in acetonitrile (AN) solutions. Here, AN is chosen as the solvent because it is a very commonly used solvent and has a medium dielectric constant of 37.5 (at 298 K) and a donor number of 14.1.<sup>15</sup> The unusually large shift of its C≡N stretch ( $\nu_2$ ) toward higher wavenumbers upon coordination with a metal cation could be used to probe the ion–solvent interactions.<sup>16–18</sup> Similar effects were found in C–C stretching.<sup>17,18</sup> The aim of this work is to study the characteristics of the interactions between each component and the structure of ion pairs, so as to gain insights into factors affecting conductivity. Therefore, the solvation structure of Li<sup>+</sup> is studied and its solvation number is calculated. Geometries and vibrational frequencies of the contact ion pairs, Li<sup>+</sup>BF<sub>4</sub><sup>−</sup> and AN–Li<sup>+</sup>BF<sub>4</sub><sup>−</sup>, and the dimers, (Li<sup>+</sup>BF<sub>4</sub><sup>−</sup>)<sub>2</sub>, are also investigated.

## Experimental Section

Lithium tetrafluoroborate (Aldrich, 98%) was recrystallized from conductivity water, followed by drying on vacuum at 353K overnight. Acetonitrile (Tianjin Reagent Factory, 99.99%, HPLC grade) was distilled under vacuum and dried over 4 Å molecular sieves. All the solutions were prepared by weight in a dry room,

\* To whom correspondence should be addressed. Tel: +86-373-3325996. Fax: +86-373-3326445. E-mail: Jwang@henannu.edu.cn.

<sup>†</sup> Henan Normal University.

<sup>‡</sup> Chinese Academy of Sciences.

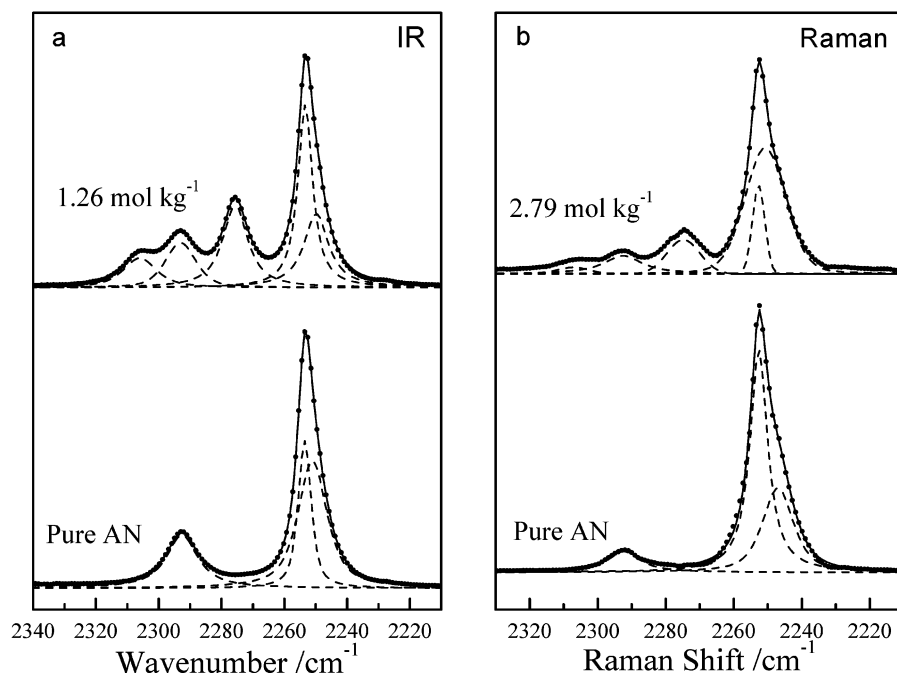


**Figure 1.** Infrared (a) and Raman (b) spectra of the C≡N stretch region of AN in LiBF<sub>4</sub>/AN solutions.

and their concentrations are expressed as molalities (mol kg<sup>-1</sup>). No significant absorption in the OH stretching region could be detected in the IR spectra, indicating that the content of water in the samples was negligible.

IR spectra were collected using a Nicolet Nexus FT-IR spectrometer with an attenuated total reflection (ATR) attachment (Spectra Tech) equipped with a ZnSe crystal in the range of 4000–600 cm<sup>-1</sup>. Raman spectra were recorded on a Raman module of the Nexus spectrometer with 1064 nm excitation from a Nd:YAG laser. The laser power was set to 300–700 mW, and 1000–2000 scans were accumulated to achieve a good signal-to-noise ratio. The liquid samples were sealed in NMR tubes and measured at room temperature (ca. 296 K). Both IR and Raman spectra were obtained with a resolution of 2 cm<sup>-1</sup>. Original spectral data were collected with Omnic 6.0 software and further processed with Win-IR 4.0 software, which fits the peaks using mixed Gaussian–Lorentzian linear combinations.

### Computational Methods

All computations in this study were made by using the Gaussian98 program.<sup>19</sup> The B3LYP set of DFT theory was chosen due to the large number of atoms involved in some of the complexes. This model has been shown in many studies to conserve disk space and be fast enough to allow the computations to be undertaken. The structures of Li<sup>+</sup> coordinated with AN were fully optimized using the 6-311++G(d,p) basis set. Initial calculations were performed on the starting geometries for BF<sub>4</sub><sup>-</sup>, Li<sup>+</sup>BF<sub>4</sub><sup>-</sup>, AN–Li<sup>+</sup>–BF<sub>4</sub><sup>-</sup>, and (Li<sup>+</sup>BF<sub>4</sub><sup>-</sup>)<sub>2</sub> based on symmetry, and preliminary studies were made at the HF level with 6-31G(d). The geometries were subsequently optimized at the B3LYP/6-311++G(d) level. Vibrational frequency calculations were performed both to confirm that the obtained structures were true minima on the potential energy surfaces and to compare with the spectroscopic data. Unless specified, the relative energies refer to those with zero-point energy (ZPE) correction. In addition, the bulk solvent effect on structures of ion pairs is also considered as a macroscopic and continuum medium using the polarized continuum models (PCM).<sup>20,21</sup>

Specifically, the polarizable dielectric model of PCM (CPCM) in Gaussian98 is used.

### Results and Discussion

**Interaction between Li<sup>+</sup> and AN Molecules.** Infrared C≡N stretches for both pure AN and AN in LiBF<sub>4</sub>/AN solutions at a salt molality of 1.26 mol kg<sup>-1</sup> are shown in Figure 1a. There are two bands for pure AN, the C≡N stretch ( $\nu_2$ ) at 2253 cm<sup>-1</sup> and the band at 2293 cm<sup>-1</sup>, which is the combination of the C–C stretch ( $\nu_4$ ) at 918 cm<sup>-1</sup> and CH<sub>3</sub> deformation ( $\nu_3$ ) at 1375 cm<sup>-1</sup>.<sup>22</sup> The shape of the IR C≡N stretch for pure AN is obviously asymmetric, and a curve fitting analysis yields a secondary band at a lower wavenumber of 2249 cm<sup>-1</sup>. Initially, this band was assigned to dimeric acetonitrile.<sup>22</sup> However, Fini and Mirone<sup>23</sup> challenged this interpretation and suggested that the secondary band is a hot band. Hot bands appear in a spectrum when the temperature increases but are unaffected by dilution. On the basis of the detailed analysis by Reimers and Hall,<sup>24</sup> the later conclusion can be adopted more easily. With the addition of LiBF<sub>4</sub>, a new band at 2276 cm<sup>-1</sup> appears and its intensity increases with increasing salt concentration. A similar change is observed for the band at 2293 cm<sup>-1</sup>. Another new band at 2306 cm<sup>-1</sup> increases in intensity at the expense of the original. The new band at 2276 cm<sup>-1</sup> is assigned to the C≡N stretch mode of the solvent coordinated to Li<sup>+</sup>, which causes a shift toward higher wavenumber by 23 cm<sup>-1</sup>. The band at 2306 cm<sup>-1</sup> is ascribed to the combination, ( $\nu_3 + \nu_4$ ), of the coordinated solvent molecule. This can be confirmed from the detailed analysis of the positions of the  $\nu_3$  and  $\nu_4$  modes in the following section.

Figure 1b shows the Raman C≡N stretch of AN with (2.79 mol kg<sup>-1</sup>) and without LiBF<sub>4</sub>. In this case, the situation is quite similar to the changes in the infrared spectra described above. Namely, two new bands appear and shift toward higher wavenumber, which are attributed to the solvent molecules directly coordinated with Li<sup>+</sup>. It is interesting to note that the magnitude of these two shifts is cation-dependent and correlated to the charge-to-radius ratio of the cation. Both the shifts of 23 and 13 cm<sup>-1</sup> are in the middle of the shifts produced by the

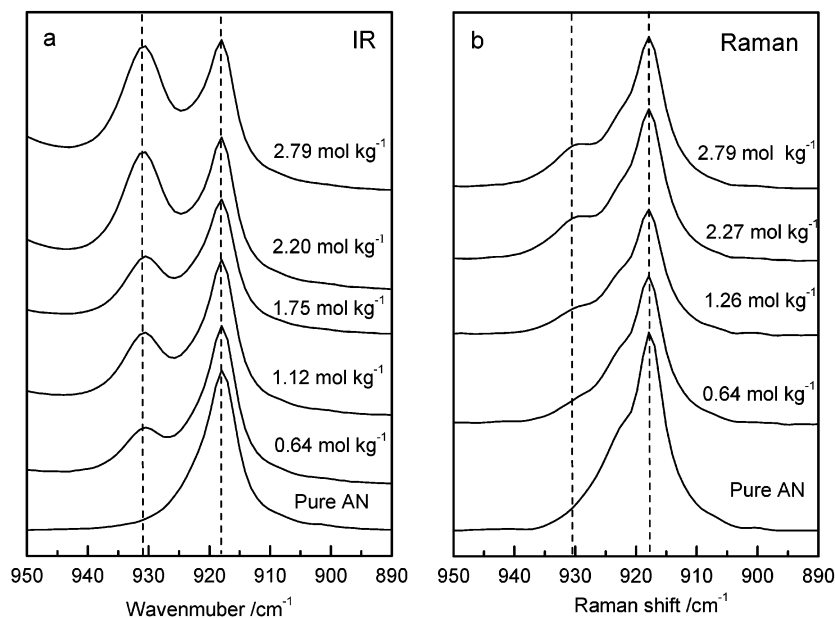


**Figure 2.** Infrared (a) and Raman (b) spectra of C–C stretch for AN as a function of the molality of LiBF<sub>4</sub>.

magnesium ion (36 and 21 cm<sup>-1</sup>)<sup>25</sup> and those corresponding to the sodium ion (13 and 5 cm<sup>-1</sup>)<sup>25,26</sup> and potassium ion (7 and 3 cm<sup>-1</sup>)<sup>25,26</sup> respectively.

Another sensitive probe for the Li<sup>+</sup>–AN interaction is the C–C stretch ( $\nu_4$ ). IR and Raman spectra in this region are shown in parts a and b of Figure 2, respectively, as a function of concentration of LiBF<sub>4</sub>. The asymmetric band at 918 cm<sup>-1</sup> is attributed to the C–C stretch ( $\nu_4$ ) mode of the free solvent molecules. A new band arising from the coordinated AN appears at 931 cm<sup>-1</sup> with the addition of LiBF<sub>4</sub>. This shift (13 cm<sup>-1</sup>) is numerically equal to the shift in position of the combination of  $\nu_3 + \nu_4$  after addition of LiBF<sub>4</sub> salt. The band at 931 cm<sup>-1</sup> increases in intensity at the expense of the band at 918 cm<sup>-1</sup>, indicating the continuous increase in the number of coordinated solvents.

On the basis of the above analysis, the strong interaction between Li<sup>+</sup> and AN is considered to have occurred through the N atom of the C≡N group of AN. On the basis of molecular orbital calculations, the molecular orbital involved in charge donation to the electrophilic species at the nitrogen end of the molecule has substantial nitrogen lone-pair character as well as C≡N and C–C antibonding contributions.<sup>27</sup> Therefore, the transfer of the electron density in this molecular orbital to a cation leads to greater bond strength in the associated vibrational models, as confirmed by the following DFT study.

It is noticeable that the Raman intensity of the  $\nu_2$  band of coordinated AN relative to that of free AN in the solutions is much lower than the corresponding IR intensity, as shown in Figure 1a,b. For example,  $I_{2276}/I_{2253}$  in the infrared spectra is nearly 4 times as high as that in Raman spectra at the salt concentration of 2.21 mol kg<sup>-1</sup>. Similar results have been reported in the study of the vibrational spectra of acrylonitrile in LiCF<sub>3</sub>SO<sub>3</sub><sup>28</sup> and AgNO<sub>3</sub><sup>16</sup> solutions. The reason for this lies in the different behaviors of the IR absorption coefficient and Raman scattering factor. The predicted value of the IR absorption coefficient of the C≡N stretch for coordinated AN is increased 10 times, while the corresponding Raman intensity is only slightly increased.<sup>29</sup> This is in agreement with our experimental results. Because the Raman intensity is linear to the concentration of the solvent, the relative intensities of the new bands, resulting from the coordinated AN, and the original

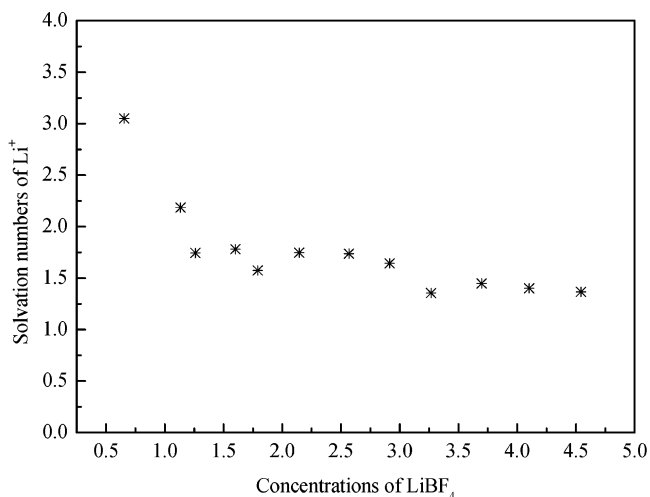


**Figure 3.** Effect of LiBF<sub>4</sub> concentrations on the solvation number of Li<sup>+</sup>.

band of free AN can be used to calculate the apparent solvation numbers by using the following relation<sup>30</sup>

$$\frac{I_c}{I_f + I_c} = N \frac{m_{\text{Li}^+}}{m_{\text{AN}}}$$

where  $I_f$  and  $I_c$  are the intensities of the bands for free and coordinated AN molecules,  $m_{\text{Li}^+}$  and  $m_{\text{AN}}$  are the concentrations of solvated lithium ions and AN molecules, and  $N$  is the average number of solvent molecules in the first solvation shell, respectively. Previous studies showed that the C≡N stretch is the most appropriate object and its molar Raman intensities are numerically the same<sup>31</sup> or slightly increased<sup>16</sup> for the solvated and bulk acetonitrile molecules. Therefore, it is acceptable that there is a direct proportionality between the band intensity and the concentration of species. To a first approximation, we used the concentration of LiBF<sub>4</sub> ( $m_{\text{LiBF}_4}$ ), instead of the concentration of the solvated Li<sup>+</sup> ( $m_{\text{Li}^+}$ ), to calculate the solvation number  $N$ . In this way, solvation numbers varying between 3.2 and 1.4 were obtained (Figure 3), depending on the concentration of salt. The solvation number of Li<sup>+</sup> is apparently lower than the

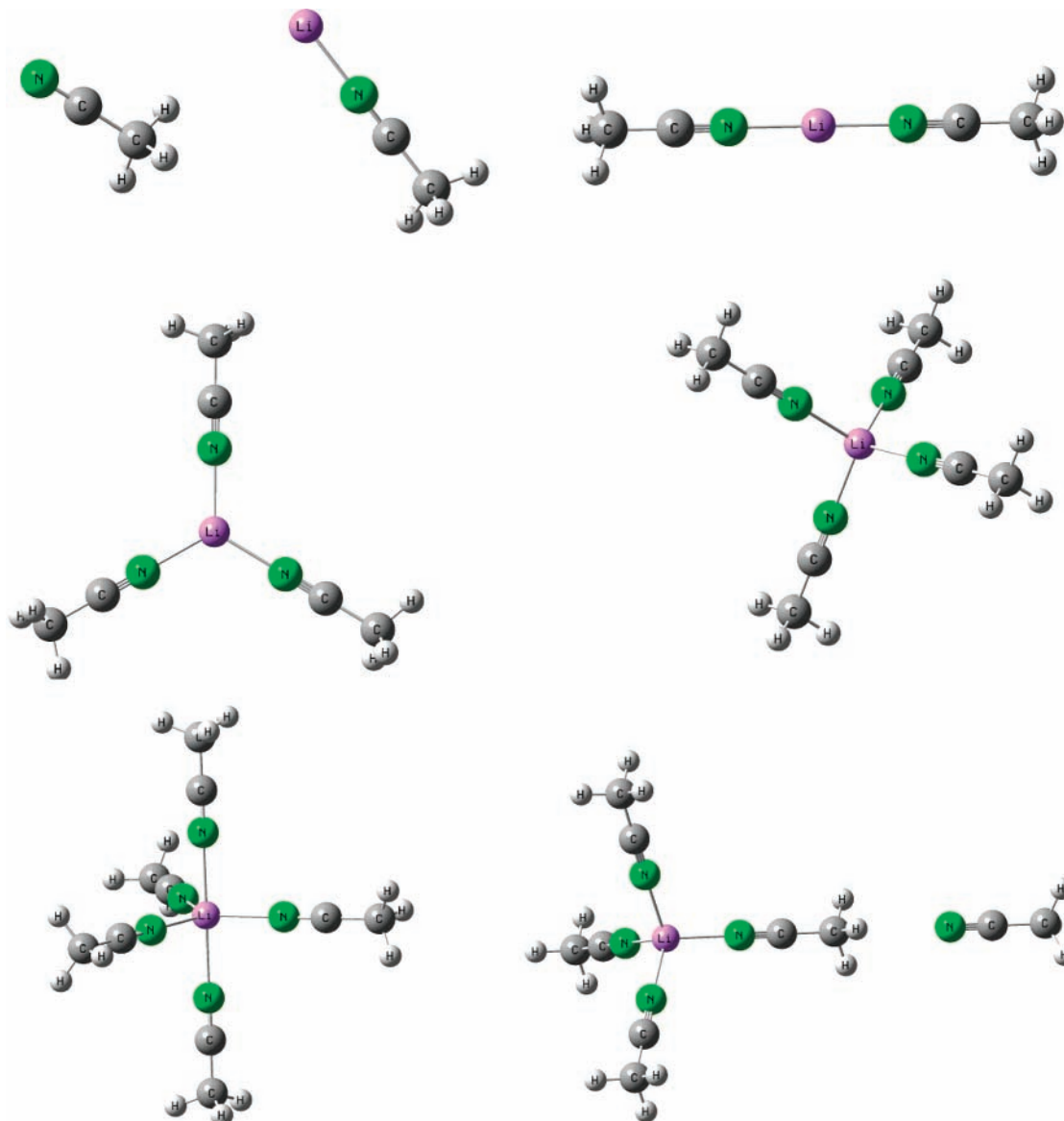


**Figure 4.** Possible structures of  $\text{Li}^+(\text{AN})_n$  ( $n = 0-5$ ) clusters as optimized by the DFT/B3LYP method.

expected one,<sup>4,5,26,32-34</sup> The reason is very clear: at the medium and high salt concentrations,  $\text{Li}^+$  has more chances to contact with the counterion and to form ion pairs, which leads to a lower concentration of the solvated  $\text{Li}^+$  and a smaller solvation number. On the other hand, it can be expected from Figure 3 that the solvation number of  $\text{Li}^+$  in AN is close to 4 in infinite diluted solutions, because ion association is negligible in this situation.

**Structure of  $\text{Li}^+$  Coordinated with AN.** Several attempts<sup>24,35-37</sup> have been made to describe the structure of liquid AN and its interaction with  $\text{Li}^+$ . Theoretical computations provide wealthy information about the properties of the clusters, including the structural features and vibrational frequencies. For this purpose, the structures of  $\text{Li}^+(\text{AN})_{1-5}$  clusters and their spectroscopic features are calculated, as shown in Figure 4 and Table 1. The structure of isolated AN has been extensively studied. The result calculated at the B3LYP/6-311++G\*\* level is very close to the experimental AN geometry, and a computed dipole moment of 4.05 D agrees very well with the experimental counterpart of 3.92 D. For the  $\text{Li}^+(\text{AN})$  cluster, the original symmetry of isolated AN molecules,  $C_{3v}$ , remains. The length of the C-N bond only shortens by 0.001 Å and the C-C bond

by 0.01 Å compared with those in the isolated AN. For  $\text{Li}^+(\text{AN})_2$ , two stable linear isomers exist. The more stable structure has a  $D_{3d}$  symmetry with methyl groups in a staggered configuration. The isomer corresponding to a  $D_{3h}$  structure with methyl groups in an eclipsed configuration has an imaginary frequency at the MP2/6-311++G\*\* level. For  $\text{Li}^+(\text{AN})_3$ , we cannot obtain its lowest energy structure because of rotation of the  $\text{CH}_3$  groups. The triangular planar configuration ( $C_{3h}$  point group), which is a minimum at the B3LYP/6-31+G\* level, is used to characterize the structure of interaction. This is acceptable, because its potential energy surface is quite flat at the minimum and the rotation of the  $\text{CH}_3$  group has little effect on energy. For the  $\text{Li}^+(\text{AN})_4$  cluster, a tetrahedral structure with a  $S_4$  symmetry is obtained. For  $\text{Li}^+(\text{AN})_5$ , the structure of five AN molecules lying in the first solvation shell is not stable. However, if four AN molecules are coordinated to  $\text{Li}^+$  in the first solvation shell and another one is in the secondary shell, a stable structure with  $C_{3v}$  point group is obtained. Moreover, the calculated value of  $\Delta G$  for the reaction  $\text{Li}^+(\text{AN})_4 + \text{AN} \rightarrow \text{Li}^+(\text{AN})_5$  is positive, while that for  $\text{Li}^+(\text{AN})_4 + \text{AN} \rightarrow \text{Li}^+(\text{AN})_4(\text{AN})$  is negative, suggesting that the solvation number of  $\text{Li}^+$  in AN solution is

**TABLE 1: Theoretical Parameters for AN Molecule and (AN)<sub>n</sub>Li<sup>+</sup> (n = 1–5) Cluster<sup>a,b</sup>**

	AN	Li <sup>+</sup> (AN)	Li <sup>+</sup> (AN) <sub>2</sub>	Li <sup>+</sup> (AN) <sub>3</sub> <sup>c</sup>	Li <sup>+</sup> (AN) <sub>4</sub>	Li <sup>+</sup> (AN) <sub>5</sub> <sup>d</sup>
<i>r</i> <sub>C–Li<sup>+</sup></sub>	–	1.8899	1.9314	1.9855	2.0508	2.0541 2.0343
<i>r</i> <sub>C–N</sub>	1.1526	1.1517	1.1509	1.1504	1.1503	1.1511 1.1502 (1.1527)
<i>r</i> <sub>C–C</sub>	1.4565	1.4470	1.4491	1.4514	1.4529	1.4519 (1.4556)
<i>r</i> <sub>C–H</sub>	1.0918	1.0926	1.0922	1.0919 1.09	1.0918	1.0917 1.0906 (1.0917)
∠CCH	110.18	109.66	109.73	109.83 109.86	109.95	110.55 109.98 109.94 (110.20)
<i>m</i>	4.05	0	0	0	0	3.24
<i>E</i> <sup>e</sup>	–132.751 046	–140.107 012	–272.914 510	–405.701 962	–538.475 565	–671.235 913
<i>ν</i> <sub>C≡N</sub>	2362	2372	2377	2382	2383	2376 (2360)
<i>ν</i> <sub>C–C</sub>	918	955	957	945	940	(938) (928)
Δ <i>ν</i> <sub>C≡N</sub> <sup>f</sup>	0	+10	+15	+23	+21	+14
Δ <i>ν</i> <sub>C–C</sub> <sup>f</sup>	0	+37	+39	+27	+22	+20
<i>N</i> <sup>g</sup>	–0.3303	+0.06378	–0.1342	+0.03368	+0.1028	+0.2101 (+0.1101)
Li <sup>+</sup> <sup>g</sup>	–	+0.6935	+0.94067	+0.5180	+0.4705	+0.4496

<sup>a</sup> Distances in angstroms, angles in degrees, dipole moment in debye, frequency in wavenumbers, and energy in hartree. <sup>b</sup> Calculated at the B3LYP/6-311++G(d,p) level. <sup>c</sup> The energy of this structure is not a minimum, because of the appearance of an imaginary frequency. However, its potential surface is very flat and this structure is close to that with the lowest energy. <sup>d</sup> Values in parentheses refer to the AN in the second solvation shell. <sup>e</sup> ZPE-corrected energy. <sup>f</sup> Δ*ν*<sub>C≡N</sub> = *ν*<sub>C≡N</sub>(calcd) – 2362; Δ*ν*<sub>C–C</sub> = *ν*<sub>C–C</sub>(calcd) – 918. <sup>g</sup> Mulliken charge.

four. This is in good agreement with the result obtained from the spectroscopic study mentioned above.

In all the cases, the interaction between Li<sup>+</sup> and AN molecules occurred through the N atom of the C≡N group. In this arrangement, the dipole of each AN molecule points directly at Li<sup>+</sup>, thereby facilitating the charge–dipole electrostatic attraction, which is primarily responsible for the overall interactions. These interactions give rise to the change of AN molecular geometry. The coordinated AN molecules nearly hold the C<sub>3v</sub> symmetry of the isolated AN, especially for Li<sup>+</sup>AN and Li<sup>+</sup>(AN)<sub>2</sub>. With an increasing number of AN molecules, the bonds of N–Li and C–C lengthen, but the reverse is true for the C–N bond. But the length of C–H remains nearly constant. The increase in the lengths of the N–Li bond from 1.890 Å in Li<sup>+</sup>(AN) to 2.054 Å in Li<sup>+</sup>(AN)<sub>5</sub> indicates the competition between the attraction of Li<sup>+</sup>–N and the repulsion in different AN molecules. The Mulliken charge on the N atom increases gradually from –0.3303 in pure AN to +0.2101 in Li<sup>+</sup>(AN)<sub>5</sub>, except for Li<sup>+</sup>(AN), revealing the transfer of charge. This can result in the shifts of the C≡N and C–C stretching modes. Additionally, the relatively high binding energy suggests the stronger electrostatic interaction between Li<sup>+</sup> and AN molecules.

Finally, we compare the experimental shifts for C≡N and C–C stretches (23 and 13 cm<sup>–1</sup>) with the calculated results. In the isolated AN, the computed positions of C≡N and C–C stretches locate at 2362 and 918 cm<sup>–1</sup>, respectively. Compared with the experimental data, the former upshifts 9 cm<sup>–1</sup>, while the latter remains unchanged. For the Li<sup>+</sup>(AN)<sub>1–4</sub> clusters, the computed position of the C≡N stretch gradually shifts toward 2383 cm<sup>–1</sup> and finally to 2376 cm<sup>–1</sup> in Li<sup>+</sup>(AN)<sub>5</sub>. The computed variation in C≡N stretch between the Li<sup>+</sup>(AN)<sub>5</sub> and the isolated AN is 14 cm<sup>–1</sup>, which is close to the experimental value. If we consider the AN in the secondary solvation shell of Li<sup>+</sup>(AN)<sub>5</sub> clusters as an isolated AN molecule, a more agreeable shift of 16 cm<sup>–1</sup> is obtained. The similarity for the shift of the C–C

stretch is also observed, and the shift of 20 cm<sup>–1</sup> is in reasonable agreement with the observed datum of 13 cm<sup>–1</sup>.

**Ion Association in AN/LiBF<sub>4</sub> Solutions.** To assess the presence of ion pairs and obtain further information on their structures, it is necessary to study the internal vibrational modes of the BF<sub>4</sub><sup>–</sup> anion. The free BF<sub>4</sub><sup>–</sup> anion belongs to the T<sub>d</sub> point group and has nine vibrational modes (A<sub>1</sub> + E + 2F<sub>2</sub>). All of them are Raman active, but the A<sub>1</sub> mode is formally forbidden in the IR. The symmetric B–F stretch (ν<sub>1</sub>) mode, is mostly used to study the ion association involving BF<sub>4</sub><sup>–</sup>, because its Raman intensity is high and the IR spectra can be activated by other species.<sup>11–14</sup> Perelygin and co-workers<sup>12</sup> studied the IR spectra of LiBF<sub>4</sub> in some dipolar aprotic solvents such as acetone and pyridine. IR analyses of the B–F symmetric stretch shown that contact ion pairs are always present in these solvents. Alía and Edwards<sup>11</sup> observed the bands at different positions in their Raman study of LiBF<sub>4</sub> or AgBF<sub>4</sub> in acrylonitrile. High association was suggested for LiBF<sub>4</sub> in this solvent. They ascribed the band at 766 cm<sup>–1</sup> to free BF<sub>4</sub><sup>–</sup>, at 773 cm<sup>–1</sup> to contact ion pairs (Li<sup>+</sup>BF<sub>4</sub><sup>–</sup>), and at 782 cm<sup>–1</sup> to the dimers (Li<sup>+</sup>BF<sub>4</sub><sup>–</sup>)<sub>2</sub>. We have also studied the solutions of NaBF<sub>4</sub> in *N,N*-dimethylformamide using Raman spectrometry<sup>38</sup> and ascribed the band at 763 cm<sup>–1</sup> to spectroscopically free anions, and the new band at 768 m<sup>–1</sup> to contact ion pairs.

Curve-fitting analyses of the IR and Raman bands of the B–F stretch in the 0.64 mol kg<sup>–1</sup> LiBF<sub>4</sub>/AN solution result in three bands located at 751, 763, and 771 cm<sup>–1</sup>, respectively, as shown in Figure 5. The band at 751 cm<sup>–1</sup> is assigned to the deformation of the C–C≡N group of AN, while the band at 763 cm<sup>–1</sup> is ascribed to the “spectroscopically free” anions,<sup>39</sup> including free BF<sub>4</sub><sup>–</sup> species and solvent-separated ion pair [Li(AN)<sup>+</sup>BF<sub>4</sub><sup>–</sup>] in which no strong interaction exists between the anion and lithium ion. The band at 771 cm<sup>–1</sup> originated from the contact ion pairs, Li<sup>+</sup>BF<sub>4</sub><sup>–</sup>. The relative intensity of I<sub>771</sub>/I<sub>763</sub> is equal to 1.90 in the IR spectrum and 2.4 in Raman spectrum, suggesting

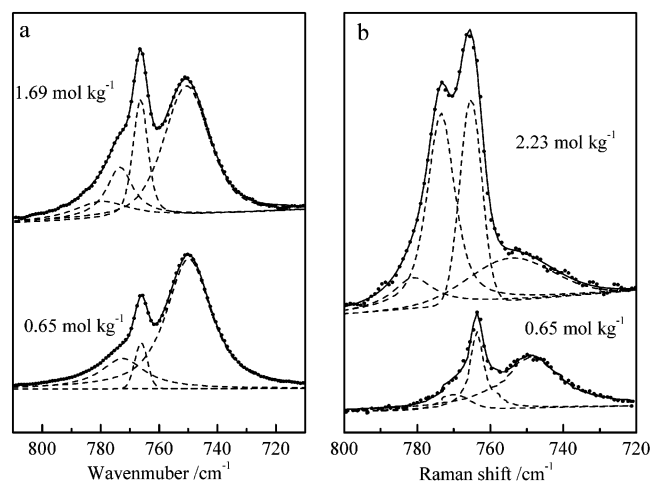


**Figure 5.** Infrared (a) and Raman (b) spectra of the  $\nu_1$  mode of  $\text{BF}_4^-$  at different concentrations of  $\text{LiBF}_4$ .

a predominance of the contact ion pairs. When the salt concentration reaches  $1.69 \text{ mol kg}^{-1}$ , a new band at  $780 \text{ cm}^{-1}$  appears and increases in intensity with increasing content of  $\text{LiBF}_4$ . This band should be ascribed to the dimer,  $(\text{Li}^+\text{BF}_4^-)_2$ . That is in accordance with the result of Alfa and Edwards.<sup>11</sup> Therefore, strong ion associations in  $\text{LiBF}_4/\text{AN}$  solutions can be inferred and spectroscopically free anions, contact ion pairs, and dimers coexist in high salt concentration solutions. Due to the presence of ion pairs in which the lithium ion is not solvated,

the concentration of solvated  $\text{Li}^+$  is smaller than that of  $\text{LiBF}_4$  used in the above calculations, leading to a smaller solvation number. No further quantitative attempt was made because of the perturbation of the deformation of  $\text{C}-\text{C}\equiv\text{N}$  group of AN in this region.

**Structure of Contact Ion Pairs and Their Dimers.** Because of the intrinsic difficulties, very few of the complete experimental studies have attempted to determine the geometries and spectroscopic features of ion pairs. As an alternative approach, ab initio methods are intensively employed to study the coordination of ion pairs in the gas state.<sup>40–43</sup> For  $\text{Li}^+\text{BF}_4^-$  contact ion pairs, three possible structures as pictured in Figure 6a–c have been suggested experimentally<sup>43</sup> and confirmed by the HF and MP2 calculations:<sup>40–43</sup> a monodenate structure (a) with a  $C_{3v}$  symmetry, a bidentate  $C_{2v}$  structure (b), and a tridentate  $C_{3v}$  structure (c). In our DFT calculations, both structures b and c are minima at the potential energy surface, and the structure a is a second-order saddle point for the sake of two imaginary frequencies. The order of stability in gas phase is  $b > c > a$ . Therefore, structure b is the geometry with the lowest energy. In this structure, the length of  $\text{F}'-\text{Li}^+$  bond is  $1.629 \text{ \AA}$ , and bond of the  $\text{B}-\text{F}'$  lengthens by  $0.167 \text{ \AA}$  compared with the  $\text{B}-\text{F}$  bond in free  $\text{BF}_4^-$ . Here, the prime indicates that the atom is the closest to the lithium ion. The computed position of the  $\text{B}-\text{F}$  symmetric stretch in structure b is at  $704 \text{ cm}^{-1}$ , which is downshift by  $-30 \text{ cm}^{-1}$  compared with the computed value ( $734 \text{ cm}^{-1}$ ) in free  $\text{BF}_4^-$  and is significantly different than the experimental result ( $+8 \text{ cm}^{-1}$ ). The same behavior is also

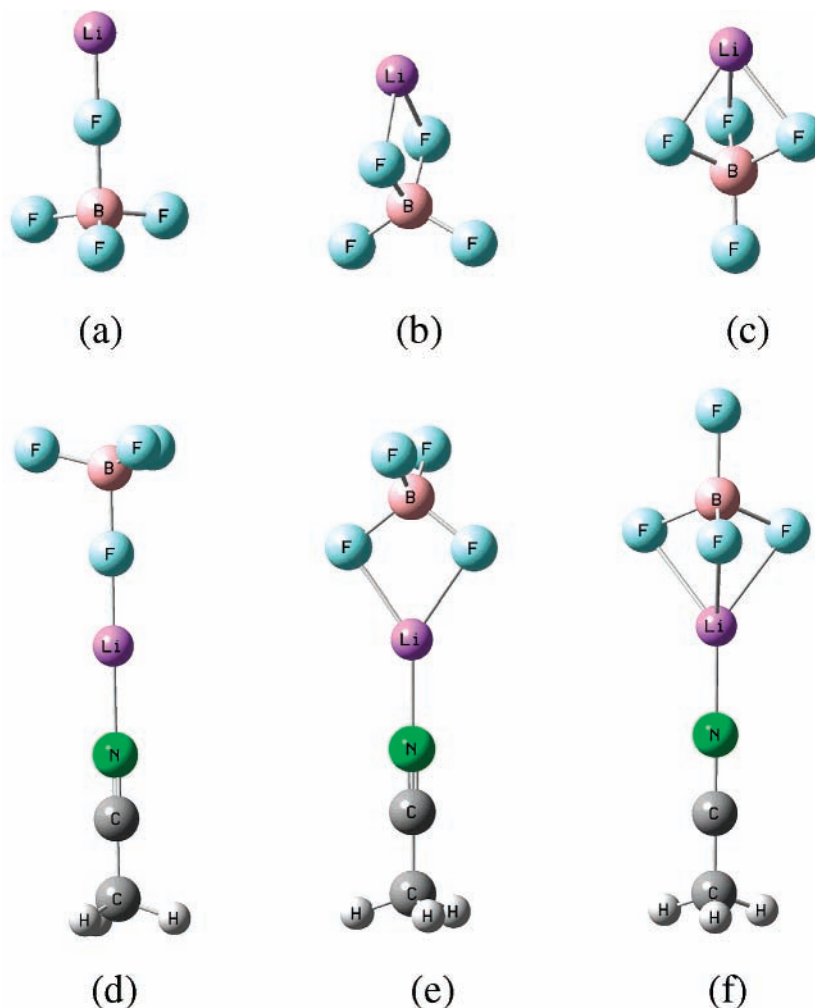


**Figure 6.** The possible structures of contact ion pairs of  $\text{Li}^+\text{BF}_4^-$ .

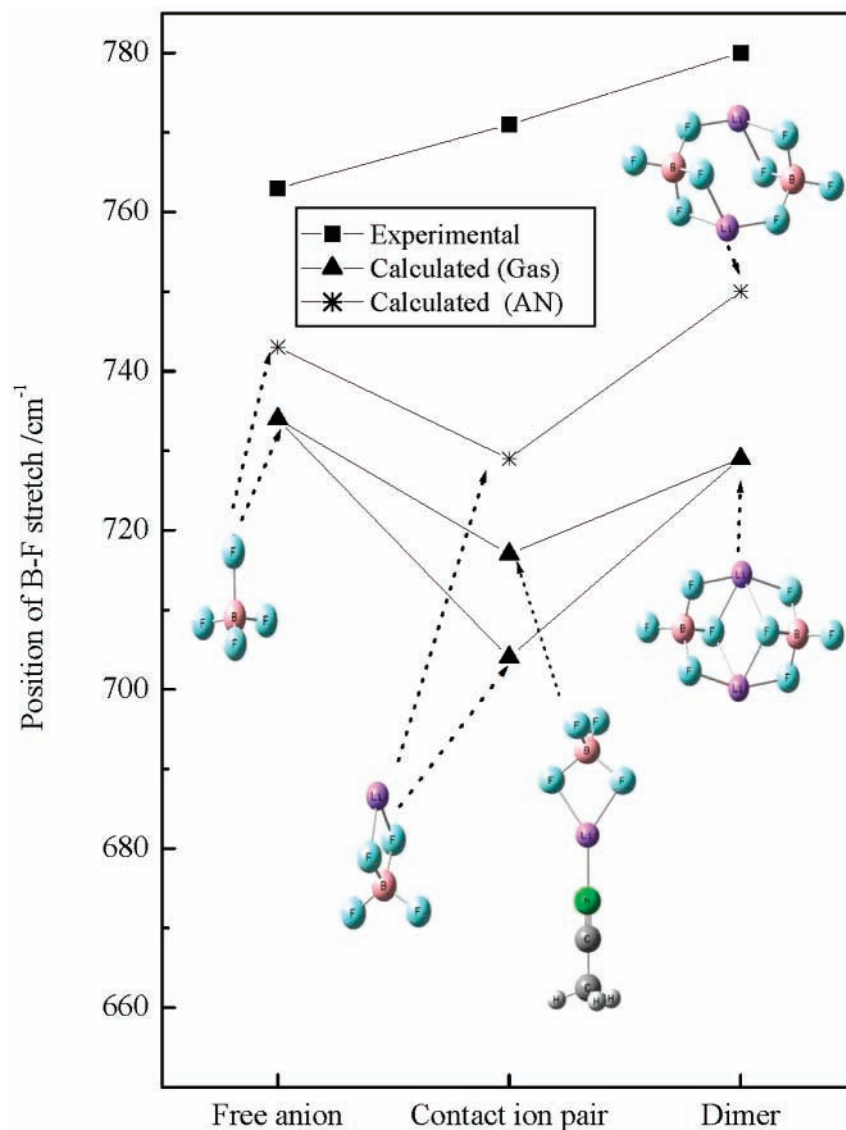


**Figure 7.** Position variations of the B–F stretch with aggregation of ions.

observed for the ClO<sub>4</sub><sup>−</sup> anion.<sup>41,44</sup> Apparently, it is not enough to account only for the cation–anion interactions, at least for reproducing the trends in the vibrational spectra. Following the idea of Johansson and Jacobsson,<sup>41</sup> we constructed a simple supermolecular structure by adding one AN molecule, coordinated with Li<sup>+</sup> through the N atom of the C≡N group, into the ion pairs as shown in Figure 6d–f to model the contact ion pairs. These structures are possible for contact ion pairs because the lithium ion can simultaneously interact with one or more AN molecules during the formation of ion pairs. It is found that structure e with C<sub>s</sub> symmetry has the lowest energy among these three structures, in which Li<sup>+</sup> interacts with one N atom of AN and two F atoms of BF<sub>4</sub><sup>−</sup>. Considering the spectroscopic features, the band of the B–F symmetric stretch located at 717 cm<sup>−1</sup> in structure e shifts considerably toward higher wavenumber by +13 cm<sup>−1</sup> relative to b, which is closer to the spectroscopic datum obtained in this work (Figure 7).

For the structure of the dimers, [Li<sup>+</sup>BF<sub>4</sub><sup>−</sup>]<sub>2</sub>, experimental hints are few in the literature. On the basis of the fact that Li<sup>+</sup>BF<sub>4</sub><sup>−</sup> is apolar or antiparallel in LiBF<sub>4</sub>/DMM solutions,<sup>10</sup> as suggested by microwave dielectric relaxation, we construct four possible structures, as shown in Figure 8g–j. Structure g and h are monodenate structures in their structural unit, and h is similar to the structure of [Li<sup>+</sup>ClO<sub>4</sub><sup>−</sup>]<sub>2</sub> proposed by Chabanel.<sup>45</sup>

However, both of them are very unstable in the gas phase because of the higher energy and presence of imaginary frequencies. Another unstable structure, i, is a mixture of the monodenate and bidenate, and the only stable structure, j, is bidenate. The geometries of the BF<sub>4</sub><sup>−</sup> in these dimer structures are severely distorted, as expected. A comparison with contact ion pairs shows the following common features for the dimers: the bond length of B–F' increased, whereas that of B–F decreased. The order of the Li<sup>+</sup>–F' bond length in dimers is found to be j > i > h > g. This order is also true for both the angle of F–B–F and for the stability of dimers. Therefore, the structure j is the most stable. Its B–F symmetric stretching mode locates at 729 cm<sup>−1</sup>, which shifts toward higher wavenumber by +12 and +25 cm<sup>−1</sup> compared respectively with those in structures e and b (Figure 7). It can be seen that the computed order for the positions of the B–F stretch, dimers > supermolecular structures > contact ion pairs, is reasonable for the ion pairs. However, compared with the B–F symmetric stretch in free BF<sub>4</sub><sup>−</sup> anion, an *upshift* of +8 and +17 cm<sup>−1</sup> was found experimentally for the contact ion pairs and their dimers, while their computed values are *downshifted*. As a result, the ion pairs in the gas phase only provide limited information about the interaction between cation and anion, and neither reproduces the observed cation-induced vibrational shifts satisfactorily.

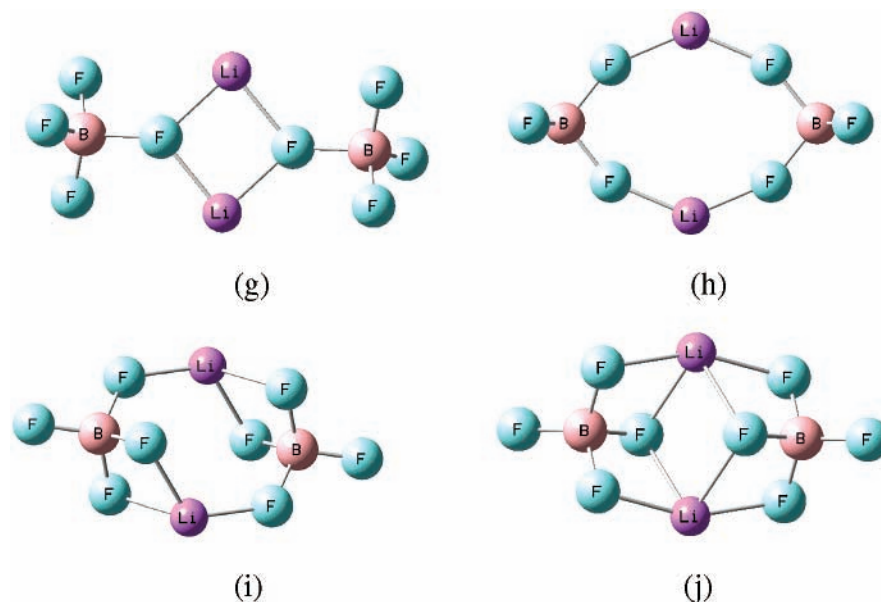


**Figure 8.** The possible structures of dimers  $[\text{Li}^+\text{BF}_4^-]_2$ .

A further study was carried out by using the PCM model<sup>20,21</sup> in Gaussian98 to model the AN solutions and to recompute the structures and vibrational frequencies of ion pairs in solutions. Insights about bulk AN solvents are provided from the CPCM calculations of the above-mentioned structures (see Figures 6 and 8). In all the cases, it is found that the bond length of B–F and  $\text{Li}^+\text{F}'$  increased, whereas that of B–F' decreased in solutions compared with those in the gas phase. Also, the angle of F–B–F increases but that of F–B–F' decreases. The stability for structures follows the order  $b > a > c$ ,  $e > d > f$  for the contact ion pairs and  $i > h > j > g$  for the dimers. It can be seen that the solvent effects change the order of stability to some extent. All of these changes demonstrate the sensitivity of those structures to solvent polarization effects. On the other hand, all the positions of the B–F symmetric stretch move toward the higher wavenumbers, which agrees better with the experimental data than those from the gas phase. However, all the structures for ion pairs, as shown in Figure 6a–f, are not theoretical minima because of the presence of imaginary frequencies. We lowered the symmetry of structure b from  $C_{2v}$  to  $C_1$  or  $C_s$  and obtained two stable structures. The  $C_s$  structure has the lowest energy and its B–F symmetric stretch locates at  $729\text{ cm}^{-1}$ . Compared with the B–F symmetric stretch ( $742\text{ cm}^{-1}$ ) in free  $\text{BF}_4^-$  in AN solvent, a downshift of  $-13\text{ cm}^{-1}$  was observed. Although this is still different in direction versus the experimental result, the change of position for the B–F symmetric stretch is closer to the experimental datum ( $+8\text{ cm}^{-1}$ ) than that in gas phase ( $-30\text{ cm}^{-1}$ ). Apparently, when only more complicated structures of contact ion pair are considered, the spectroscopic feature of the contact ion pair in AN solution could be reasonably predicted. For dimers of structure g–j in AN solutions, the solvent effect changes the order of stability, and structure i is most stable. The predicted shift of the B–F symmetric stretch (at  $750\text{ cm}^{-1}$ ) in this structure is  $+9\text{ cm}^{-1}$  relative to that in free  $\text{BF}_4^-$  in AN solvent, which is in excellent agreement with the experimental result ( $+8\text{ cm}^{-1}$ ).

## Conclusions

Vibrational spectroscopies and DFT calculations are proved useful for understanding the ion solvation and association of  $\text{LiBF}_4$  in AN solutions as a function of the concentration of the

lithium salt. The following tentative conclusions can be drawn from the present studies:

(1) Strong interactions between  $\text{Li}^+$  and the N atoms of the  $\text{C}\equiv\text{N}$  groups of AN molecules are responsible for the structural changes of AN. This interaction affects the  $\text{C}\equiv\text{N}$  stretching mode and results in the transfer of an electron from the N atom of the  $\text{C}\equiv\text{N}$  group to  $\text{Li}^+$ , as shown by the decrease of cation charge with increasing cluster size. The greatest contribution to this interaction is the electrostatic component. The solvation number of lithium ion in  $\text{LiBF}_4/\text{AN}$  solutions varies with the concentrations of the salt and is found to be 4 in the *infinitely diluted* solutions. The solvation shell of  $\text{Li}^+$  saturates with four AN molecules because of the smaller cation radius, and the fifth AN molecule will be squeezed out of the solvation shell, as shown in Figure 4.

(2) Ion association is high at medium and high salt concentrations, as can be deduced from the vibrational band changes of the B–F symmetric stretch in  $\text{BF}_4^-$  anions. The observed three bands in this region,  $763$ ,  $771$ , and  $780\text{ cm}^{-1}$ , are assigned to the spectroscopically free anions, contact ion pairs, and dimers, respectively. Ion association reduces the number of solvated  $\text{Li}^+$  and leads to a smaller solvation number.

(3) The bidentate structure with  $C_{2v}$  symmetry for contact ion pairs formed by  $\text{Li}^+$  and  $\text{BF}_4^-$  is the most preferred in the gas phase. The addition of one AN molecule to  $\text{Li}^+\text{BF}_4^-$  strongly affects the structural parameters, but not the order of stability. Three possible structures for the dimers are constructed for the first time. It is shown that the energy of the structure with  $C_{2h}$  point group, in which one  $\text{Li}^+$  interacts with two F atoms of two  $\text{BF}_4^-$  anions, is the minima of potential energy surface. The calculations for the positions of the B–F stretch based on these structures predict a reasonable order of shift in wavenumber, but significant discrepancies were found from the experimental values. Considering the solvent effect, the bidentate structure with  $C_s$  point group for contact ion pairs and the structure i, a mixture of the monodentate and bidentate structures, for dimers are the most stable. Good agreement was found between the experimental and theoretical spectroscopic changes of the B–F symmetric stretch.

**Acknowledgment.** Financial support from the National Natural Science Foundation of China (No. 29973009) and the



Innovation Foundation of Henan Education Department is gratefully acknowledged.

## References and Notes

- (1) Zhang, S. S.; Xu, K.; Jow, T. R. *J. Electrochem. Soc.* **2002**, *149*, A586.
- (2) Winter, M.; Besenhard, J. O. In *Lithium Ion Batteries: Fundamentals and Performances*; Wakihara, M.; Yamamoto, O., Ed.; Academic Press: New York, 1999.
- (3) Muhuri, P. K.; Hazra, D. K. *J. Chem. Soc., Faraday Trans.* **1991**, *87*, 3511.
- (4) Tsunekawa, H.; Narumi, A.; Sano, M.; Hiwara, A.; Fujita, M.; Yokoyama, H. *J. Phys. Chem. B* **2003**, *107*, 10962.
- (5) Chagnes, A.; Carré, B.; Willmann, P.; Lemordant, D. *J. Power Sources* **2002**, *109*, 203.
- (6) Das, B.; Hazra, D. K. *J. Phys. Chem.* **1995**, *99*, 269.
- (7) Delsignore, M.; Maaser, H.; Petrucci, S. *J. Phys. Chem.* **1984**, *88*, 2405.
- (8) Maaser, H.; Delseignore, M.; Newstein, M.; Petrucci, S. *J. Phys. Chem.* **1984**, *88*, 5100.
- (9) Muhuri, P. K.; Das, B.; Hazra, D. K. *J. Phys. Chem. B* **1997**, *101*, 3329.
- (10) Delsignore, M.; Farber, H.; Petrucci, S. *J. Phys. Chem.* **1986**, *90*, 66.
- (11) Alía, J. M.; Edwards, H. G. M. *J. Solution Chem.* **2000**, *29*, 781.
- (12) Pereygin, I. S.; Klimchuk, M. A. *Russ. J. Phys. Chem.* **1989**, *63*, 143.
- (13) Pereygin, I. S.; Klimchuk, M. A.; Plakhotnik, V. N.; Tovmash, N. *F. Russ. J. Phys. Chem.* **1988**, *62*, 928.
- (14) Frech R.; Manning J. P. *Electrochem. Acta* **1992**, *37*, 1499.
- (15) Marcus Y. In *Ion Solvation*; Wiley: Chichester, 1985.
- (16) Alía, J. M.; Edwards, H. G. M.; Moore, J. *Spectrochim. Acta* **1995**, *51A*, 2039.
- (17) Seo, J.; Kim, K.; Cho, H.; *Spectrochim. Acta* **2003**, *59A*, 477.
- (18) Cha, J.; Cheong, B.; Cho, H.; *J. Phys. Chem. A* **2001**, *105*, 1789.
- (19) Frisch, M. J.; Trucks, G. W.; Schlegel, H. B.; Scuseria, G. E.; Robb, M. A.; Cheeseman, J. R.; Zakrzewski, V. G.; Montgomery, J. A.; Stratmann, Jr. R. E.; Burant, J. C.; Dapprich, S.; Millam, J. M.; Daniels, A. D.; Kudin, K. N.; Strain, M. C.; Farkas, O.; Tomasi, J.; Barone, V.; Cossi, M.; Cammi, R.; Mennucci, B.; Pomelli, C.; Adamo, C.; Clifford, S.; Ochterski, J.; Petersson, G. A.; Ayala, P. Y.; Cui, Q.; Morokuma, K.; Rega, N.; Salvador, P.; Dannenberg, J. J.; Malick, D. K.; Rabuck, A. D.; Raghavachari, K.; Foresman, J. B.; Cioslowski, J.; Ortiz, J. V.; Baboul, A. G.; Stefanov, B. B.; Liu, G.; Liashenko, A.; Piskorz, P.; Komaromi, I.; Gomperts, R.; Martin, R. L.; Fox, D. J.; Keith, T.; Al-Laham, M. A.; Peng, C. Y.; Nanayakkara, A.; Challacombe, M.; Gill, P. M. W.; Johnson, B.; Chen, W.; Wong, M. W.; Andres, J. L.; Gonzalez, C.; Head-Gordon, M.; Replogle, E. S.; Pople, J. A. *Gaussian 98*, Revision A.11; Gaussian, Inc., Pittsburgh, PA, 2002.
- (20) Miertus, S.; Scrocco, E.; Tomasi, J. *Chem. Phys.* **1981**, *55*, 117.
- (21) Miertus, S.; Tomasi, J. *Chem. Phys.* **1982**, *65*, 239.
- (22) Loewenschuss, A.; Yellin, N. *Spectrochim. Acta* **1975**, *31A*, 207.
- (23) Fini, G.; Mirone, P. *Spectrochim. Acta* **1976**, *32A*, 439.
- (24) Reimers, J.; Hall, E. L. *J. Am. Chem. Soc.* **1999**, *121*, 3730.
- (25) Fawcett, W. R.; Liu, G. *J. Phys. Chem.* **1992**, *96*, 4231.
- (26) Fawcett, W. R.; Liu, G.; Faguy, P. W.; Foss, C. A.; Motheo, A. J. *J. Chem. Soc., Faraday Trans.* **1993**, *89*, 811.
- (27) Vigay, A.; Sathyanarayana, D. N. *J. Phys. Chem.* **1996**, *100*, 75.
- (28) Alía, J. M.; Edwards, H. G. M.; Mera, Y. D.; Lawson, E. E. *J. Solution Chem.* **1997**, *26*, 497.
- (29) Sadlej, J. *Spectrochim. Acta* **1979**, *35A*, 681.
- (30) Balasubrahmanyam, K.; Janz, G. J. *J. Am. Chem. Soc.* **1970**, *92*, 4189.
- (31) Oliver, B. G.; Janz, G. J. *J. Phys. Chem.* **1970**, *74*, 3819.
- (32) Barthel, J.; Buchner, R.; Wismeth, E. *J. Solution Chem.* **2000**, *29*, 937.
- (33) Seo, J.; Cheong, B.; Cho, H. *Spectrochim. Acta* **2002**, *58A*, 1747.
- (34) Loring, J. S.; Fawcett, W. R. *J. Phys. Chem. A* **1999**, *103*, 3608.
- (35) Cabaleiro-Lago, E.; Ríos, M. *J. Phys. Chem. A* **1997**, *101*, 8327.
- (36) Cabaleiro-Lago, E.; Ríos, M. *Chem. Phys.* **2000**, *254*, 11.
- (37) Siebers, J. G.; Buck, U.; Beu, T. A. *Chem. Phys.* **1998**, *239*, 549.
- (38) Xuan, X.; Zhang, H.; Wang, J.; Wang, H. *J. Raman Spectrosc.* **2003**, *34*, 465.
- (39) Alía, J. M.; Edwards, H. G. M.; Moore, J. *J. Chem. Soc., Faraday Trans.* **1996**, *92*, 1187.
- (40) Francisco, J. S.; Willams, I. H. *J. Phys. Chem.* **1990**, *94*, 8522.
- (41) Johansson, P.; Jacobsson, P. *J. Phys. Chem. A* **2001**, *105*, 8504.
- (42) Spoliti, M.; Sanna, N.; Martino, V. D. *J. Mol. Struct. (THEOCHEM)* **1992**, *258*, 83.
- (43) Borodin, O.; Smith, G. D.; Douglas, R. *J. Phys. Chem. B* **2003**, *107*, 6824.
- (44) Klassen, B.; Aroca, R.; Nazri, G. A. *J. Phys. Chem.* **1996**, *100*, 9334.
- (45) Chabanel, M.; Legoff, D.; Touaj, K. *J. Chem. Soc., Faraday Trans.* **1996**, *92*, 4205.